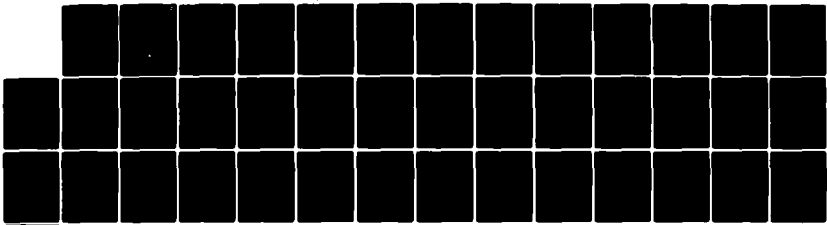
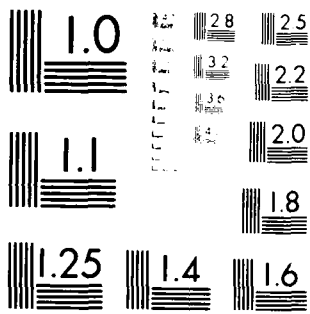


AD-A134 458 THE EVOLUTION OF SPONTANEOUS AND COHERENT RADIATION IN 1/1
THE FREE ELECTRON LASER OSCILLATOR(U) NAVAL RESEARCH
LAB WASHINGTON DC P SPRANGLE ET AL. 16 AUG 83
UNCLASSIFIED NRL-MR-5110 F/G 20/5 NL



END
DATE
FILMED
11-83
DTIC



MICROCOPY RESOLUTION TEST CHART
 NATIONAL BUREAU OF STANDARDS-1963-A

2

NRL Memorandum Report 5110

A134 458

The Evolution of Spontaneous and Coherent Radiation in the Free Electron Laser Oscillator

P. SPRANGLE, C. M. TANG AND I. BERNSTEIN*

*Plasma Theory Branch
Plasma Physics Division*

**Yale University
New Haven, CT*

August 16, 1983

This work was supported by DARPA under contract No. 3817.

DTIC FILE COPY



NAVAL RESEARCH LABORATORY
Washington, D.C.

DTIC
ELECTE
NOV 07 1983

[Handwritten signature]

Approved for public release; distribution unlimited.

88 11 04 050

20 ABSTRACT (Continued)

rate equation, which described the evolution of the radiation pulses within the resonator. The wiggler field is assumed to occupy a portion of the finite Q resonator. In the energy rate equation, the spontaneous (incoherent) radiation term is represented by a source matrix, while the stimulated (coherent) radiation term is represented by a gain matrix. The effect of small variations in the mirror separation are investigated in the context of laser lethargy. Our analysis suggests possible methods which could substantially shorten the start-up times in FEL oscillators. Finally, our results are compared with the FEL oscillator experiments performed at Stanford University.

CONTENTS

I. Introduction..... 1

II. FEL Oscillator Start Up Model..... 4

III. Reduced Wave Equation..... 5

IV. Particle Dynamics..... 9

V. Radiation Dynamics..... 12

VI. Derivation of Energy Rate Equation..... 14

VII. Reduced Energy Rate Equation..... 17

VIII. Spontaneous Radiation Source Term..... 22

IX. Long Beam Pulse Limit..... 24

X. Numerical Illustrations, Experimental Comparison
and Discussion..... 26

Acknowledgment..... 34

References..... 35

| | |
|---------------|---|
| Accession No. | |
| NTIS GRA&I | X |
| DTIC TAB | |
| Unannounced | |
| Justification | |

A-1



THE EVOLUTION OF SPONTANEOUS AND COHERENT RADIATION IN THE FREE ELECTRON LASER OSCILLATOR

I. Introduction

A number of successful free electron laser oscillator experiments have been reported.¹⁻⁴ Simple considerations concerning the spontaneous radiation level indicated start-up times much shorter than those observed.³ Since a number of experiments utilizing shorter electron beam macropulses are being constructed or planned, thus, there is concern that these forthcoming experiments may be unable to reach saturation. A quantitative understanding of the growth of coherent stimulated radiation from incoherent spontaneous emission is thus highly desirable. Published papers on the FEL oscillator had either neglected the spontaneous radiation⁵⁻²⁰, or had treated them separately from the stimulated radiation.¹³ Here we outline a classical theory of the spontaneous start-up of the FEL oscillator in the cold, small signal regime. Our model is spatially one dimensional and therefore lacks many important features such as transverse gradients associated with the radiation and electron beam and diffraction effects. In a one-dimensional model these effects can only be incorporated in an approximate way by means of filling factors.

Theories⁵⁻²⁸ of the free electron laser (FEL) have proceeded from a continuum description of the electron dynamics, either fluid equations or the Vlasov equation. For a proper description of the start-up of an FEL oscillator one must take into account the fact that the electrons are discrete and initially uncorrelated, since it is the acceleration radiation of individual electrons in the wiggler that provides the initial fields. These initial fields are then amplified by the collective gain mechanism associated with the continuum description. This initial radiation, however, is effectively incoherent in a device in which the electron density is small and the electrons are randomly

Manuscript approved May 23, 1983.

distributed. Thus a statistical theory is required which is couched in terms of objects bilinear in the fluctuating quantities so that ensemble averages are non-zero, even when the ensemble average fluctuating current density is zero.

The theory described in this work is one dimensional in space and treats the electrons as governed by the relativistic equations of motion, and the electromagnetic fields as governed by Maxwell's equations. This is valid whenever the root mean square fluctuation $\delta\bar{N}$ in the number of photons in the resonator is small compared with the mean number of photons \bar{N} . Certainly this is not true initially, and in principle, one should treat the problem initially by quantum mechanics. Failure to do so implies an uncertainty in the initial phases of the start up. Since one expects $\delta\bar{N} \sim (\bar{N})^{1/2}$ if the electrons are randomly distributed, the duration of the quantum regime will be short if classical theory predicts for times short compared to that for saturation that the photon density $N = \int d^3r (\underline{E}^2 + \underline{B}^2)/(4h \omega_L) \gg 1$, where $\omega_L = 2 \gamma^2 c k_w$ is the laser frequency, and h is Planck's constant.

This paper presents an analysis of the transition from the incoherent radiation to the coherent radiation²⁹ in an FEL oscillator. The model of the FEL oscillator is described in Sec. II. The equations governing the complex amplitude of the radiation in terms of the particle trajectories are derived in Sec. III; and the equations governing the particle trajectories in terms of the radiation field are derived in Sec. IV. The results of Secs. III and IV are combined in Sec. V to obtain the self-contained radiation dynamics equations. The equation describing the dynamics of the radiation energy rate matrix is derived in Sec. VI. The solution of the energy rate equation is obtained in Sec. VII. The three-dimensional effects of the spontaneous radiation are incorporated into the one-dimensional model through a filling factor in Sec. VIII. The analysis of the FEL

oscillator start-up process is now completed. We examine a limiting case, in Sec. IX, where the electron pulse length is long. In the final section, Sec. X, we compare our numerical results with Stanford's FEL oscillator data. Finally in this section a number of possible methods are suggested to shorten the FEL oscillator's start-up time.

II. FEL Oscillator Start Up Model

The schematic representation of the FEL oscillator model used in our analysis is shown in Fig. 1. The resonator defined by plane reflectors at $z = 0$ and $z = L$ contains the wiggler magnetic field located between $z = L_0$ and $z = L_0 + L_w$. The total resonator losses are modeled heuristically by a Q factor. The highly relativistic pulsed electron beam enters the resonator from the left at $z = 0$ with axial velocity $v_0 \hat{e}_z$. Within the wiggler field the axial pulse velocity is reduced slightly to $v_{0z} \hat{e}_z$. The electron beam pulses are spatially periodic with period L_b . Though L_b is arbitrary in the analysis, it is clear that for proper matching between the beam and radiation pulses that, L_b should be approximately an integer times $2v_0L/c$. The radiation pulse in the wiggler field, when overlapping with the beam pulse, can travel at a velocity slightly less than c , and the effect is called laser lethargy. It, therefore, becomes necessary to slightly mistune (shorten) the resonator length to optimize the interaction. This effect is fully taken into account and is discussed in detail later. The axial profile of the electron beam pulses are left arbitrary but have a characteristic length $l_b \ll L_b$. The entering electron beam is monoenergetic with no spread in either the longitudinal or transverse velocities. The radiation pulse is assumed to undergo little change in phase and amplitude during a single pass through the resonator, i.e., low gain operating regime. The wiggler parameters are taken to be fixed and space charge effects neglected. Finally the analysis is performed in the small signal regime, i.e., to first order in the radiation field.

III. Reduced Wave Equation

We will represent the radiation field within the resonator by a superposition of spatial modes, which are such that the tangential electric field vanishes on the mirrors. The vector potential of the radiation field is written as

$$\tilde{A}_R(z, t) = \sum_{n=1}^{\infty} a_n(t) \sin(k_n z) e^{i\omega_n t} \hat{e}_x + c.c. \quad (1)$$

where $k_n = \omega_n/c = n\pi/L$, $a_n(t)$ is the Fourier coefficient of the n th mode, and $c.c.$ denotes the complex conjugate. The vector potential of the linearly polarized wiggler field is non-zero only in the interval $L_0 \leq z \leq L_0 + L_w$ and is taken to be

$$\tilde{A}_w(z) = A_w \cos(k_w z) \hat{e}_x \quad (2)$$

where $k_w = 2\pi/\ell_w$, ℓ_w is the wiggler wavelength and $|\tilde{A}_w| \gg |\tilde{A}_R|$. The one-dimensional wave equation for \tilde{A}_R , including a phenomenological loss term, is

$$\left(\frac{\partial^2}{\partial z^2} - \frac{1}{c^2} \frac{\partial^2}{\partial t^2} - \frac{\nu}{c^2} \frac{\partial}{\partial t} \right) \tilde{A}_R(z, t) = -\frac{4\pi}{c} \tilde{J}(z, t) \quad (3)$$

where the current density \tilde{J} will eventually be taken to be linear in \tilde{A}_R , $\nu = \omega_L/Q$, ω_L is the characteristic laser frequency, and Q is the quality factor associated with the resonator. In the FEL the characteristic laser frequency is $\omega_L = (1 + \beta_{oz}^2) \gamma_{oz}^2 v_{oz} k_w$, where $\beta_{oz} = v_{oz}/c$ and $\gamma_{oz} = (1 - \beta_{oz}^2)^{-1/2}$. In (3) the Q is defined in the usual way such that in the absence of a driving current the electromagnetic stored energy (proportional to $|a_n(t)|^2$) decays like $\exp(-\omega_L t/Q)$. Note that in (3) it is assumed that all the significantly excited longitudinal modes have the same Q .

The actual discrete beam density is

$$n(z,t) = \frac{1}{\sigma_b} \sum_{j=1}^N \delta [z - \tilde{z}(z_{0j}, t)] \quad (4)$$

and σ_b is the cross sectional area of the electron beam and $\tilde{z}(z_{0j}, t)$ represents the axial orbit of the j th electron. At $t=0$ the initial axial position of the j th electron is z_{0j} , i.e., $\tilde{z}(z_{0j}, t=0) = z_{0j}$.

The fluid like beam density can be defined as

$$n_o(z,t) = \langle n(z,t) \rangle \quad (5)$$

where the bracket $\langle \rangle$ denotes the ensemble average of the enclosed quantity.

The ensemble average in (5) is over uncorrelated charged sheets (electrons).

Using (4) we note that the ensemble average of the density $n(z,t)$ is

$$\langle \frac{1}{\sigma_b} \sum_{j=1}^N \delta(z - \tilde{z}(z_{0j}, t)) \rangle = \int dz_o n_o(z_o, 0) \delta(z - \tilde{z}(z_o, t)) = n_o(z,t) \quad (6)$$

where $n_o(z_o, 0)$ is the initial spatial density distribution of particles. The fluctuating part of the density is given by $n(z,t) - \langle n(z,t) \rangle$. The effective non-linear driving current density is given by

$$\tilde{J}(z,t) = \tilde{J}_c(z,t) + \tilde{J}_{inc}(z,t) \quad (7a)$$

where \tilde{J}_c is the coherent current driving the stimulated radiation (gain) and \tilde{J}_{inc} is the incoherent contribution due to the discrete nature of the electrons and is responsible for the spontaneous radiation (shot noise). The coherent and incoherent current densities are respectively given by

$$\tilde{J}_c = - |e| v_w F_c \langle n(z,t) \rangle \quad (7b)$$

and

$$\tilde{J}_{inc} = - |e| v_w F_{inc} [n(z,t) - \langle n(z,t) \rangle] \quad (7c)$$

where

$$v_w = c \beta_w = |e| A_w(z) / \gamma_o m_o c = v_w \cos(k_w z) \hat{e}_x \quad (8)$$

is the wiggler velocity defined over the region $L_o \leq z \leq L_o + L_w$, $v_w = |e| A_w / (\gamma_o m_o c)$ and $\gamma_o = (1 - v_o^2/c^2)^{-1/2}$. The usual filling factor associated with the coherent radiation is $F_c = \sigma_b / \sigma_r$, where σ_r is the transverse area of the resonator radiation mode. The filling factor associated with the incoherent radiation is written as $F_{inc} = \sqrt{f_m} \sqrt{\xi}$. The term f_m is a loss factor due to the finite size of the mirror at $z=L$ and is given by $f_m = [2\gamma_o r_m / (1 + \gamma_o \beta_w) L]^2$ where r_m is the mirror radius. In obtaining f_m we have taken the incoherent radiation divergence angle to be $\approx (1/\gamma_o + \beta_w)$. The origin of the second term in the expression for F_{inc} arises from the one dimensional statistics performed on the uncorrelated particles. In Sec. VIII we show that this term is given by $\xi = \sigma_b (\gamma_o / \gamma_{oz})^6 / (\lambda_L \gamma_{oz})^2$ where $\lambda_L = \ell_w (1 + \beta_{oz})^{-1} \gamma_{oz}^{-2}$ is the characteristic laser wavelength.

It should be emphasized that in our model the electrons are actually represented by sheets of charge. The surface charge of each sheet is $-|e|/\sigma_b$ and the sheets (electrons) are taken to be uncorrelated.

To obtain an equation for $a_n(t)$, the Fourier coefficients of the radiation field, we first substitute (1) together with (7) and (8) into the wave equation (3). Taking $a_n(t)$ to be a slowly varying function of time, i.e., $|\dot{a}_n/a_n| \ll \omega_n$, there results on neglecting small terms

$$\begin{aligned}
& -2i \sum_{n=1}^{\infty} \frac{\omega_n}{c} \left[\dot{a}_n(t) + \frac{v}{2} a_n(t) \right] \sin k_n z e^{i\omega_n t} + \text{c.c.} \\
& = 4\pi |e| \beta_w \cos k_w z \left(\frac{F_{\text{inc}}}{\sigma_b} \sum_{j=1}^{\infty} \delta(z - z(\tilde{z}_{oj}, t)) - (F_{\text{inc}} - F_c) n_o(z, t) \right) \\
& \theta(z - L_o) \theta(L_o + L_w - z)
\end{aligned} \tag{9}$$

where $\beta_w = v_w/c$ is the normalized wiggler velocity, $\theta(x)$ is the usual Heaviside unit step function, and the dot denotes a time derivative. By multiplying both sides of (9) by $\sin k_m z$, integrating over z from 0 to L , and keeping the appropriate resonant terms we obtain

$$\begin{aligned}
\dot{a}_n(t) &= \frac{-v}{2} a_n(t) + \frac{\pi |e| v_w}{k_n L} \int_0^L dz e^{i(k_n + k_w)z - i\omega_n t} \\
& \left(\frac{F_{\text{inc}}}{\sigma_b} \sum_{j=1}^{\infty} \delta(z - \tilde{z}(z_{oj}, t)) - (F_{\text{inc}} - F_c) n_o(z, t) \right) \\
& \theta(z - L_o) \theta(L_o + L_w - z).
\end{aligned} \tag{10}$$

To evaluate $a_n(t)$, knowledge of the axial orbit, i.e., $\tilde{z}(z_{oj}, t)$, is required.

IV. Particle Dynamics

The longitudinal particle dynamics are governed primarily by the ponderomotive force resulting from the beating of the radiation and wiggler field, see for example Refs. 21-27. Keeping only the ponderomotive term which is bilinear in A_w and A_R and neglecting space charge effects, we find that the axial dynamics of the j th electron in the wiggler region, $L_0 \leq z \leq L_0 + L_w$ is given by

$$\ddot{\tilde{z}}(z_{0j}, t) = - \left(\frac{|e|}{\gamma_0 m_0 c} \right)^2 \left(\frac{\partial}{\partial z} + \frac{v_{oz}}{c^2} \frac{\partial}{\partial t} \right) \left(A_w(z) \cdot A_R(z, t) \right) \Big|_{z=\tilde{z}_j} \quad (11)$$

where v_{oz} is the axial electron velocity in the wiggler. By substituting (1) and (2) into (11) and keeping the appropriate resonant terms on the right hand side of (11) we obtain

$$\ddot{\tilde{z}}(z_{0j}, t) = - \left(\frac{|e| \beta_w k_w}{2 \gamma_0 m_0} \right) \left[\sum_{n=1}^{\infty} a_n(t) e^{-i(k_n + k_w)z - \omega_n t} + c.c. \right] \quad (12)$$

$0(z - L_0) \quad 0(L_0 + L_w - z)$

where the right hand side of (12) is evaluated at $z = \tilde{z}(z_{0j}, t)$ and we have made use of the approximation $(1 - \beta_{oz}) k_n + k_w \approx 2 k_w$. Within the wiggler field the axial electron velocity in the absence of the radiation field as determined by conservation of energy is

$$v_{oz} = v_0 (1 - \beta_w^2/4), \quad (13)$$

where v_0 is the axial electron velocity prior to entering the wiggler field. The trajectory of the j th electron prior to entering the wiggler field is

$$\tilde{z}(z_{0j}, t) = z_{0j} + v_0 t \quad (14)$$

where $t \leq (L_0 - z_{0j})/v_0$. Within the wiggler the trajectory of the j th electron is

$$\tilde{z}(z_{0j}, t) = \tilde{z}^{(0)}(z_{0j}, t) + \delta\tilde{z}(z_{0j}, t) \quad (15)$$

where $\tilde{z}^{(0)}(z_{0j}, t) = v_{oz} z_{0j}/v_0 + (1 - v_{oz}/v_0) L_0 + v_{oz} t$ is the unperturbed orbit and $\delta\tilde{z}$ is the displacement due to the ponderomotive force. Equations (12) and (15) are valid for times such that the particle is in the wiggler, i.e., $(L_0 - z_{0j})/v_0 \leq t \leq (L_0 - z_{0j})/v_0 + L_w/v_{oz}$. Substituting (15) into (12) and linearizing we find that the longitudinal displacement of the j th electron satisfies

$$\begin{aligned} \ddot{\delta\tilde{z}}(z_{0j}, t) = & - \left(\frac{|e| \beta_w k_w}{2\gamma_0 m_0} \right) \sum_{n=1}^{\infty} a_n(t) e^{-i(k_n + k_w)(z'_{0j} + L_0 - L'_0)} e^{-i\mu_n t} \\ & + \text{c.c.} \left[0 \left(\frac{z_{0j} - L_0}{v_0} + t \right) \right] \left[0 \left(\frac{L_0 - z_{0j} + L'_w}{v_0} - t \right) \right] \end{aligned} \quad (16)$$

where $\beta_{oz} = v_{oz}/c$, $\mu_n = v_{oz}(k_n + k_w) - \omega_n = v_{oz}k_w - c k_n(1 - \beta_{oz})$ is the frequency mismatch, $z'_{0j} = v_{oz} z_{0j}/v_0$, $L'_0 = v_{oz} L_0/v_0$ and $L'_w = v_0 L_w/v_{oz}$. We now invoke the low gain assumption by taking the coefficients $a_n(t)$ to be constant during the time the j th electron is within the wiggler region. Integrating (16) twice, using the low gain assumption, and taking the initial conditions such that the relative displacement and relative displacement velocity are zero at the entrance to the wiggler, i.e., $\delta\tilde{z} = \dot{\delta\tilde{z}} = 0$ at $t = (L_0 - z_{0j})/v_0$, we find that

$$\delta\tilde{z}(z_{0j}, t) = \left(\frac{|e| \beta_w k_w}{2\gamma_0 m_0} \right) \sum_{m=1}^{\infty} a_m(t) \mu_m^{-2} e^{-i(k_m + k_w)(z'_{0j} + L_0 - L'_0)}$$

$$\left[e^{-i\mu_m t} + (i\mu_m \left(t - \frac{(L_o - z_{oj})}{v_o} \right) - 1) e^{-i\mu_m (L_o - z_{oj})/v_o} \right] + \text{c.c.} \quad (17)$$

where expression (17) is valid for times such that $(L_o - z_{oj})/v_o \leq t \leq (L_o + L_w - z_{oj})/v_o$ and is zero prior to this time interval. Expression (10) together with (17) describes the linear, low gain, longitudinal dynamics of the j th particle within the wiggler field.

V. Radiation Dynamics

We now return to the evolution of the radiation field. Substituting (15) together with (17) into (10), introducing coefficients $b_n(t) = k_n a_n(t)$, and expanding the delta functions, the expression for the time rate of change of the Fourier coefficients is given by

$$\dot{b}_n(t) = -\frac{\nu}{2} b_n(t) + \tilde{S}_n(t) + R_n(t) \quad (18)$$

where

$$\tilde{S}_n(t) = \frac{\pi |e| v_w F_{inc}}{L \sigma_b} \int_{L_0}^{L_0 + L_w} dz e^{i(k_n + k_w)z - i\omega_n t} \left(\sum_{j=1} \delta(z - \tilde{z}^{(o)}(z_{oj}, t)) - \sigma_b n_o(z, t) \right), \quad (19a)$$

$$R_n(t) = \frac{\pi |e| v_w F_c}{L} \int_{L_0}^{L_0 + L_w} dz e^{i(k_n + k_w)z - i\omega_n t} n_o(z, t) \quad (19b)$$

and $\delta\tilde{z}(z_{oj}, t)$ is given by (17). On the right hand side of (18), the first term represents the resonator losses, $\tilde{S}_n(t)$ represents the spontaneous or incoherent radiation term, and the stimulated or coherent radiation is represented by $R_n(t)$. Substituting the linearized, low gain, longitudinal orbit of the j th particle within the wiggler field given by (17) into (6) the stimulated term in (18) can be expressed as

$$R_n(t) = \sum_{m=1}^{\infty} \tilde{G}_{nm}(t) b_m(t) \quad (20)$$

where

$$\check{G}_{nm}(t) = \frac{i\pi |e|^2 v_w^2 k F_c}{2\gamma_o m_o c L} e^{i(\mu_n - \mu_m)t} e^{i(k_n - k_m)(L_o - L_o')} \mu_m^{-2} \int_{L_o - v_o t}^{L_o + L_w' - v_o t} dz_o n_o(z_o, 0) e^{i(k_n - k_m)v_{oz} z_o / v_o} \left\{ 1 + [i\mu_m(t - (L_o - z_o)/v_o) - 1] e^{i\mu_m(t - (L_o - z_o)/v_o)} \right\} \quad (21)$$

where $L_w' = L_w v_o / v_{oz} \approx L_w$. The time rate of change of the Fourier amplitude given in (18) can therefore be put into the form

$$\dot{b}_n(t) = \check{S}_n(t) + \sum_{m=1}^{\infty} (\check{G}_{nm}(t) - \frac{\nu}{2} \delta_{nm}) b_m(t) \quad (22)$$

where $\check{S}_n(t)$ is the spontaneous radiation source term, $\check{G}_{nm}(t) b_m(t)$ represents the dielectric response or gain, δ_{nm} is the Kronecker delta, and $(\nu/2) \delta_{nm} b_m(t)$ is the loss term due to the finite Q of the resonator. The matrix $\check{\underline{G}}$ defined by the elements $\check{G}_{nm}(t)$ will be referred to as the gain matrix.

VI. Derivation of Energy Rate Equation

The total ensemble average electromagnetic energy within the resonator is

$$W_{em}(t) = \int_{vol} d^3r \langle \tilde{E}^2 + \tilde{B}^2 \rangle / 8\pi = \frac{\sigma_R L}{4\pi} \sum_{n=1}^{\infty} \langle b_n b_n^* \rangle \quad (23a)$$

and the electromagnetic power flowing axially within the resonator is

$$P_{em}(z,t) = \frac{c}{4\pi} \int_{area} dA \langle \tilde{E} \times \tilde{B} \rangle = \frac{c\sigma_R}{16\pi} \sum_{n,m=1}^{\infty} \langle b_n b_m^* \rangle \left[e^{-i(k_n - k_m)(z - ct)} - e^{i(k_n - k_m)(z + ct)} \right] \hat{e}_z + c.c. \quad (23b)$$

where the bracket $\langle \rangle$ denotes the ensemble average over uncorrelated sheets (electrons) of the enclosed quantity. From (23a) and (23b) it is clear that the quantity of real interest is the energy density matrix $\underline{\epsilon}$ defined by the elements

$$\epsilon_{nm}(t) = \langle b_n(t) b_m^*(t) \rangle. \quad (24)$$

In terms of the energy density matrix in (24), the total electromagnetic energy, W_{em} , and the electromagnetic power, $P_{em}(z,t)$, are

$$W_{em}(t) = \frac{\sigma_R L}{4\pi} \sum_{n=1}^{\infty} \epsilon_{nn}(t) \quad (25a)$$

and

$$P_{em}(z,t) = \frac{c\sigma_R}{16\pi} \sum_{n,m=1}^{\infty} \epsilon_{nm}(t) \left[e^{-i(k_n - k_m)(z - ct)} - e^{i(k_n - k_m)(z + ct)} \right] \hat{e}_z + c.c. \quad (25b)$$

We now derive the rate equation for the energy density matrix. Writing (22) in vector notation yields

$$\dot{\underline{b}}(t) = \underline{\tilde{S}}(t) + [\underline{\tilde{G}}(t) - \frac{\nu}{2} \underline{I}] \underline{b}(t) \quad (26)$$

where \underline{I} is the unit matrix. Solving (26), with initial condition $\underline{b}(0) = 0$, we obtain

$$\underline{b}(t) = \int_0^t \underline{X}(t) \underline{X}^{-1}(t') \underline{\tilde{S}}(t') dt' \quad (27)$$

where $\underline{X}(t)$ is defined by the equation

$$\dot{\underline{X}}(t) = [\underline{\tilde{G}}(t) - \frac{\nu}{2} \underline{I}] \underline{X}(t) \quad (28)$$

with initial conditions $\underline{X}(0) = \underline{I}$. The energy density matrix is

$$\underline{\epsilon}(t) = \langle \underline{b}(t) \underline{b}^H(t) \rangle \quad (29)$$

where $\text{Trace}(\underline{\epsilon}) = (\sigma_R L)^{-1} \int d^3r \langle E_{\underline{c}}^2 + B_{\underline{c}}^2 \rangle / 2$ and the superscript H denotes the Hermitian conjugate. Using (27) together with (29) we find that $\underline{\epsilon}(t)$ satisfies the rate equation

$$\dot{\underline{\epsilon}}(t) = [\underline{\tilde{G}}(t) - \nu \underline{I}] \underline{\epsilon}(t) + \underline{\dot{\Sigma}}(t) + \text{H.C.} \quad (30)$$

where $\underline{\dot{\Sigma}}(t) = \int_0^t \langle \underline{\tilde{S}}(t) \underline{\tilde{S}}^H(t') \rangle (\underline{X}(t) \underline{X}^{-1}(t'))^H dt'$

and H.C. denotes the Hermitian conjugate of the preceding terms. It can be shown

that the ensemble average of $S_n(t) S_m^*(t)$ can be expressed as

$$\langle \tilde{S}_n(t) \tilde{S}_m^*(t') \rangle = \left(\frac{\pi |e| v_w}{L} \right)^2 \frac{F_{inc}^2}{\sigma_b} e^{i\mu_n t} e^{-i\mu_m t'} e^{i(k_n - k_m)(L_o - L_o')} \\ \int_{L_o - v_o t}^{L_o + L_w' - v_o t} dz_o n_o(z_o, 0) e^{i(k_n - k_m)v_{oz} z_o / v_o} \\ \Theta(z_o - L_o + v_o t') \Theta(L_o + L_w' - z_o - v_o t') \quad (31)$$

By noting the limits of integration as well as the arguments of the Heaviside functions in (31), it is clear that the ensemble average $\langle \tilde{S}_n(t) \tilde{S}_m^*(t) \rangle$ is non-zero only for $t - t' \leq L_w / v_{oz}$, i.e., when there is an electron sheet in the wiggler. It can be shown that in this interval $\underline{X}(t) \underline{X}^{-1}(t') \approx \underline{I}$ if the gain per pass is somewhat less than unity. Hence the source term of the energy rate Eq. (30) is simplified to

$$\dot{\underline{Y}}(t) \approx \int_0^t \langle \tilde{S}(t) \tilde{S}^H(t') \rangle dt' \quad (32)$$

The elements of (32) take the form

$$\dot{Y}_{nm}(t) = i \left(\frac{\pi |e| v_w}{L} \right)^2 \frac{F_{inc}^2}{\sigma_b} e^{i(\mu_n - \mu_m)t} e^{i(k_n - k_m)(L_o - L_o')} \\ \int_{L_o - v_o t}^{L_o + L_w' - v_o t} dz_o n_o(z_o, 0) e^{i(k_n - k_m)v_{oz} z_o / v_o} \mu_m^{-1} \left(1 - e^{i\mu_m(t - (L_o - z_o)/v_o)} \right) \quad (33)$$

$$\int_{L_o - v_o t}^{L_o + L_w' - v_o t} dz_o n_o(z_o, 0) e^{i(k_n - k_m)v_{oz} z_o / v_o} \mu_m^{-1} \left(1 - e^{i\mu_m(t - (L_o - z_o)/v_o)} \right)$$

This completes our formal derivation of the energy rate equation given by (30).

VII. Reduced Energy Rate Equation

Due to the complicated structure of both the gain matrix (21) as well as the spontaneous source matrix (33), it is convenient to further reduce these terms to a more manageable form. To this end we define a time variable t_N , such that t_N is the time that the center of the Nth electron pulse enters the wiggler field, that is

$$t_N = ((N - 1) L_b + L_o) / v_o \quad (34)$$

where N is a non zero positive integer. During the electron pulse propagation through the wiggler field, the independent time variable is

$$t = t_N + \tau$$

where $0 \leq \tau \leq L_w / v_{oz}$. To simplify the gain matrix and spontaneous source matrix in (21) and (33) we note that these matrices involve integrals of the general form

$$I_{nm}(t) = \int_{L_o - v_o t}^{L_o + L_w - v_o t} dz_o n_o(z_o) e^{i(k_n - k_m) v_{oz} z_o / v_o} F_{nm}(t, z_o). \quad (35)$$

The generic integral in (35) can be evaluated for two representative electron pulse shapes of characteristic width ℓ_b given

$$I_{nm}(t_N + \tau) = F_{nm}[t_N + \tau, - (N-1)L_b] n_o \ell_b e^{-i(k_n - k_m) (N-1) v_{oz} L_b / v_o} \rho_{nm} \quad (36)$$

where

$$\rho_{nm} = \frac{\sqrt{\pi}}{2} e^{-((k_n - k_m) \ell_b / 4)^2}, \quad \text{Gaussian profile} \quad (37a, b)$$

$$\rho_{nm} = \frac{\sin((k_n - k_m) \ell_b / 2)}{(k_n - k_m) \ell_b / 2}, \quad \text{square profile.}$$

The expression in (37a) is for a Gaussian electron beam pulse shape, i.e.,

$$n_o(z_o) = n_o e^{-(2 z_o/\ell_b)^2} \quad (38a)$$

while the expression in (37b) is for a square pulse shape, i.e.,

$$n_o(z_o) = \begin{cases} n_o, & -\ell_b/2 \leq z_o \leq \ell_b/2, \\ 0, & \text{otherwise.} \end{cases} \quad (38b)$$

Using the result contained in (36), together with (34), both the gain matrix and the spontaneous source matrix can be reduced to

$$\begin{aligned} \tilde{G}_{nm}(t_N + \tau) &= \frac{i}{8} \frac{\ell_b}{L} \frac{\omega_b^2}{\gamma_o} \beta_w^2 k_w^2 F_c e^{-i(k_n - k_m)(N-1)L_b} \\ &\frac{\alpha_{nm} \rho_{nm}}{2 \mu_m} e^{i(\mu_n - \mu_m)\tau} (1 + (i\mu_m \tau - 1) e^{i\mu_m \tau}) \end{aligned} \quad (39a)$$

and

$$\begin{aligned} \tilde{L}_{nm}(t_N + \tau) &= \frac{i\pi}{4} \frac{\ell_b}{L} \frac{\omega_b^2 m_o}{L\sigma_b} v_w^2 F_{inc}^2 e^{-i(k_n - k_m)(N-1)L_b} \\ &\frac{\alpha_{nm} \rho_{nm}}{\mu_m} e^{i(\mu_n - \mu_m)\tau} (1 - e^{i\mu_m \tau}) \end{aligned} \quad (39b)$$

where

$$\alpha_{nm} = \exp(-i(k_n - k_m)(1 - \beta_o)\beta_o^{-1}L_o)$$

and $\omega_b^2 = 4\pi|e|^2 n_o/m_o$ is the peak beam plasma frequency. In obtaining (39a) and (39b) we replaced $v_{oz} \ell_b/v_o$ by ℓ_b .

In the absence of "laser lethargy" exact resonance between the electron beam pulses and the radiation pulses occur when the mirror separation is equal to $L_b/(2\beta_0)$ where β_0 is the normalized axial pulse velocity outside the wiggler field. This condition implies that the round trip of the radiation pulse, if it were traveling at c , equals the beam pulse period. However, since the radiation pulse velocity, in the wiggler region when overlapping with the electron pulse, is slightly less than c , it is necessary to have the mirror separation slightly less than $(L_b/2\beta_0)$ for optimum overlap of the beam and radiation pulses.⁵⁻¹⁹ With this in mind we define the mirror separation to be

$$L = L_m + \delta L \quad (40)$$

where $L_m \equiv L_b/(2\beta_0) \gg |\delta L|$. In (38) and (39) the only term sensitive to slight variations in the mirror separation is the common leading term $\exp(-i(k_n - k_m)(N-1)L_b)$. Substituting (40) into (39a) and (39b) and assuming δL small we find that the gain and source matrix elements become

$$\tilde{G}_{nm}(t_N + \tau) = \frac{1}{8} \frac{\ell_b}{L} \frac{\omega_b^2}{\gamma_0} \beta_w^2 k_w c F_c \alpha_{nm} \rho_{nm} e^{2i\pi(n-m)(N-1)\delta L/L_m} \frac{e^{i(\mu_n - \mu_m)\tau}}{\mu_m^2} (1 + (i\mu_m\tau - 1) e^{i\mu_m\tau}) \quad (41)$$

and

$$\lambda_{nm}(t_N + \tau) = \frac{\ell_b}{L} \frac{\pi^2 |e|^2 n_0 v_w^2}{L \sigma_h} \alpha_{nm} \rho_{nm} F_{inc}^2 e^{2i\pi(n-m)(N-1)\delta L/L_m} \tau e^{i(\mu_n - \mu_m)\tau} e^{i\mu_m\tau/2} \left(\frac{\sin \mu_n \tau/2}{\mu_n \tau/2} \right). \quad (42)$$

The rate of change of the field energy density matrix given in (30), together with the expressions for \tilde{G}_{nm} and $\dot{\gamma}_{nm}$ in (41) and (42), can be still further reduced by invoking the low gain per pass approximation. The low gain per pass assumption implies that $\underline{\epsilon}$ changes slightly during a single pass of the radiation pulse. Hence, by taking $\underline{\epsilon}(t_N + \tau)$, where $\tau \leq L_w/v_{oz}$, to be nearly equal to $\underline{\epsilon}(t_N)$ on the right hand side of (30), we can integrate (30) together with (41) and (42). Doing this we find that the elements of $\underline{\epsilon}$ at time $t_N + \tau$ are given approximately by

$$\begin{aligned} \epsilon_{nm}(t_N + \tau) &\approx (1 - \nu \tau) \epsilon_{nm}(t_N) + S_{nm}(t_N, \tau) \\ &+ \sum_{\ell=1}^{\infty} \{G_{n\ell}(t_N, \tau) \epsilon_{\ell m}(t_N) + \epsilon_{n\ell}(t_N) G_{m\ell}^*(t_N, \tau)\} \end{aligned} \quad (43)$$

where

$$\begin{aligned} G_{nm}(t_N, \tau) &= \int_0^{\tau} \tilde{G}_{nm}(t_N + \tau') d\tau' \\ &= \frac{-1}{32} \frac{\ell_b}{L} \frac{\omega_b^2}{\gamma_o} \beta_w^2 k_w c F_c e^{2i\pi(n-m)(N-1)\delta L/L_m} \alpha_{nm} \rho_{nm} g_{nm}(\tau) \end{aligned} \quad (44a)$$

and

$$\begin{aligned} S_{nm}(t_N, \tau) &= \int_0^{\tau} (\dot{\gamma}_{nm}(t_N + \tau') + \text{H.C.}) d\tau' \\ &= \frac{\ell_b}{2L} \frac{\pi^2 |e|^2 n_o v_w^2}{L \sigma_b} F_{inc}^2 e^{2i\pi(n-m)(N-1)\delta L/L_m} \alpha_{nm} \rho_{nm} h_{nm}(\tau) \end{aligned} \quad (44b)$$

where

$$g_{nm}(\tau) = \frac{\tau^3}{x_n x_m} \left(e^{ix_n} \left(1 + \frac{x_m}{x_n} \right) \sin x_n - e^{i(x_n - x_m)} x_n \left(\frac{\sin(x_n - x_m)}{x_n - x_m} \right) - x_m e^{2ix_n} \right), \quad (45a)$$

and

$$h_{nm}(\tau) = \frac{\tau^2}{x_n x_m} \left[\sin^2 x_n + \sin^2 x_m - \sin^2(x_n - x_m) - i \left[\sin x_n \cos x_n - \sin x_m \cos x_m - \sin(x_n - x_m) \cos(x_n - x_m) \right] \right], \quad (45b)$$

and $x_n = \mu_n \tau / 2 = [v_{oz} k_w - ck_n(1 - v_{oz}/c)]\tau/2$. Note that since h_{nm} is Hermitian, so is the spontaneous source matrix S_{nm} in (44b). The fact that S_{nm} is Hermitian is simply a consequence of the fact that r_{nm} by definition is Hermitian, (see (24)). Setting $\tau = L_w/v_{oz}$ in (43) gives the energy density matrix after the N th beam pulse has transversed the wiggler. The results obtained by numerically solving (43) for various experimental parameters will be presented later.

VIII. Spontaneous Radiation Source Term

The spontaneous radiation source term in (44b) has been obtained from a one dimensional analysis of the wave equation. Because of the one-dimensional character of the analysis the spontaneous source term does not properly represent the incoherent radiation source. A proper three-dimensional treatment of the spontaneous radiation is necessary to properly consider the statistics of discrete uncorrelated particles as well as to separate the "velocity" and "acceleration" (radiation) electromagnetic fields.³⁰ The present one dimensional treatment represents the electrons as uncorrelated charged sheets and not as point particles. To correct for the one-dimensional limitations of our analysis of the spontaneous source term we have included in the incoherent current density (7c), a filling factor which contains the term $\sqrt{\epsilon}$. This term is included so that the total emitted spontaneous radiation agrees with the well known value obtained from Larmor's formula. We have justified this procedure by performing a proper three-dimensional treatment of the spontaneous source term; this three-dimensional analysis will be published elsewhere. To obtain the factor ϵ in the spontaneous source term, i.e., in the filling factor F_{inc} , we compare the total emitted radiation energy from (43) with that obtained from Larmor's formula with the loss terms f_m set equal to unity and $v = 0$. From (43), the diagonal elements of $\underline{\epsilon}$ satisfy

$$\epsilon_{nn}(t_N + \tau) = 2 \frac{\ell_b}{L} \frac{\pi^2 |e|_n^2 v_w^2}{L \sigma_b} F_{inc}^2 \frac{\sin \mu_n \tau}{\mu_n} \quad (46)$$

where we have used the expression for ρ_{nm} in (44b) and are considering a square shaped electron beam pulse, i.e., $\rho_{nn} = 1$. We now want to compare (46) with Larmor's radiative formula. The total instantaneous power radiated³⁰ from a single particle is

$$P_{em}^L = \frac{2}{3} \frac{|e|^2}{c^3} \gamma_o^6 (\dot{\underline{v}}^2 - (\underline{v} \times \dot{\underline{v}})). \quad (47)$$

The velocity of a single particle in the wiggler is $\underline{v} = v_{oz} \hat{e}_z + v_w \cos(k_w v_{oz} t) \hat{e}_x$. Using (47) we find that the total energy radiated during a time $\tau \leq L_w/v_{oz}$, by a beam pulse consisting of $\ell_b n_o \sigma_b$ particles, is

$$W_{em}^L = \frac{1}{3} \frac{|e|^2}{c} \frac{\gamma_o^6}{\gamma_{oz}} \ell_b n_o \sigma_b (\beta_{oz} k_w v_w)^2 \tau. \quad (48)$$

The total spontaneous electromagnetic energy within the resonator is given by (25a) with σ_R replaced by σ_b . Substituting (46) into (25a) gives

$$W_{em}(t_N + \tau) = \frac{\sigma_b L}{4\pi} \int_1^\infty dn \int_0^{\tau \leq L_w/v_{oz}} \frac{d\tau}{\tau} \left(\frac{2\ell_b}{L} \frac{\pi^2 |e|^2 n_o^2 v_w^2}{L \sigma_b} F_{inc}^2 \right) \frac{\sin \mu_n \tau}{\mu_n} + W_{em}(t_N) \quad (49)$$

where we have approximated the sum by an integral. Integrating (49) over τ and n gives

$$W_{em}(t_N + \tau) = W_{em}(t_N) + \frac{\pi}{2} \frac{|e|^2}{c} \frac{\ell_b n_o^2 v_w^2}{(1 - \beta_{oz})} F_{inc}^2 \tau. \quad (50)$$

Comparing (48) and (50) we find that, for $f_m = 1$,

$$F_{inc}^2 = \xi = \left(\frac{\gamma_o}{\gamma_{oz}} \right)^6 \frac{\sigma_b}{(\lambda_L \gamma_{oz})^2} \quad (51)$$

where λ_L is the laser wavelength, $\lambda_L = \ell_w / (1 + \beta_{oz}) \gamma_{oz}^2$.

IX. Long Beam Pulse Limit

A limiting case which can be fully evaluated analytically is that of a long pulse beam, i.e., $l_b \lesssim L$. Though this limit is not necessarily directly applicable to either planned or completed pulsed beam FEL oscillator experiments it does represent an interesting limit of the more realistic configurations. If the electron pulse widths are comparable but somewhat less than the mirror separation, L , the gain matrix as well as the spontaneous source matrix in (44a) and (44b) approach a diagonal form. This can be seen by noting that for $l_b \lesssim L$, the matrix defined by ρ_{nm} and used in (44a) and (44b) approaches $(\sqrt{\pi}/2) \delta_{nm}$ for a Gaussian beam pulse and δ_{nm} for a square shape beam pulse where δ_{nm} is the Kronecker delta. The diagonal form of (44a) and (44b) is reasonable in this limit, since it is the off diagonal elements, in particular the term $\exp(2\pi i(n-m)(N-1)\delta L/L_m)$, which are responsible for the laser lethargy effect and when the beam width is sufficiently long this effect is unimportant. In this limit a single longitudinal mode analysis would suffice.

Therefore, the energy rate equation in (43) together with (44a) and (44b), for long beam pulses, takes the form

$$\epsilon_{nn}(t_N + \tau) \approx (1 - \nu \tau + \tilde{g}_{nn}(\tau)) \epsilon_{nn}(t_N) + S_{nn}(\tau) \quad (52)$$

where the diagonal gain and source matrix elements are respectively

$$\begin{aligned} \tilde{g}_{nn}(\tau) &= G_{nn}(t_N + \tau) + G_{nn}^*(t_N + \tau) \\ &= -\frac{1}{16} \frac{l_b \omega_b^2}{L \gamma_0} \beta_w^2 k_w^2 c F_c^3 \tau^3 \frac{\partial}{\partial x_n} \left(\frac{\sin x_n}{x_n} \right)^2 \end{aligned} \quad (53a)$$

$$S_{nn}(\tau) = \frac{l_b}{L} \frac{\pi^2 |e|_n^2 v_w^2}{L \sigma_b} F_{inc}^2 \left(\frac{\sin x_n}{x_n} \right)^2 \tau^2 \quad (53b)$$

and $x_n = \mu_n \tau / 2$. In obtaining (53) we have assumed a square pulse shape. Note that in $\tilde{g}_{nn}(\tau)$ and $S_{nn}(\tau)$, τ ranges from 0 to L_w/v_{oz} . Since ϵ_{nn} changes little from pulse to pulse we may transform (52) into a first order temporal differential equation. Since $t_{N+1} = t_N + L_b/v_o$, (52) can be written as

$$\frac{d\epsilon_{nn}(t)}{dt} = \{\tilde{g}_{nn}/\Delta t - v\} \epsilon_{nn}(t) + S_{nn}/\Delta t \quad (54)$$

where $\Delta t = 2L_b/v_o$, \tilde{g}_{nn} and S_{nn} are to be evaluated at $\tau = L_w/v_{oz}$ and we have replaced the discrete time parameter t_N with the continuous parameter t .

Integrating (54) yields

$$\epsilon_{nn}(t) = \frac{S_{nn}}{\tilde{g}_{nn} - v\Delta t} (e^{(\tilde{g}_{nn} - v\Delta t)t/\Delta t} - 1) \quad (55)$$

where $\epsilon_{nn}(t=0) = 0$. For times less than a growth time, i.e., $t < \Delta t/(\tilde{g}_{nn} - v\Delta t)$,

$$\epsilon_{nn}(t) = S_{nn} (t/\Delta t + (\tilde{g}_{nn} - v\Delta t)t^2/2\Delta t^2). \quad (56)$$

X. Numerical Illustrations, Experimental Comparison and Discussion

Our numerical illustrations are directed towards a comparison of the FEL oscillator experimental results reported in Ref. 4. In addition, we suggest methods, which could substantially shorten the oscillator start-up time.

The parameters of Stanford's FEL oscillator is given in Table I. In the FEL oscillator experiment a helical wiggler field was used. Since the present analysis assumes a linear wiggler it becomes necessary to multiply B_w in Table I by $\sqrt{2}$ in order to be consistent. The peak power within the resonator as a function of the number of beam pulses that have passed through the resonator is shown in Fig. 2 for six values of the resonator mismatch length $\delta L = L_m - L_b/2\beta_0$. Figure 3 shows the asymptotic gain as a function of δL . The mirror mismatch $\delta L = -1.1 \times 10^{-3}$ cm corresponds to maximum gain but not maximum saturated power. Maximum saturated power occurs for δL between 0 and -1.1×10^{-3} cm. The range in δL for nonzero gain is -3.0×10^{-3} cm $< \delta L < 0$, in fair agreement with the experimental range of 2.5×10^{-3} cm. The maximum calculated multi-mode (finite beam pulse) power gain is 0.16 whereas the single mode (continuous beam) yields a value of 0.25. Finite beam pulse effects therefore reduce the linear gain by approximately 60%. The maximum experimental gain is 0.10.

Figure 4 shows the spatial distribution of the electron pulse (square) and the radiation power pulses at the entrance and exit of the wiggler for $\delta L = -1.0 \times 10^{-3}$ cm. Upon entering the wiggler the radiation pulse slightly lags the beam pulse, while exiting the wiggler the two are completely overlapped. The asymptotic energy spectrum of the radiation, Fig. 5, is narrower and shifted with respect to the spontaneous radiation spectrum.

Equation (43) suggests that one can roughly compute the relationship between P_N , the peak power in the resonator after the Nth pulse, to P_0 , the power emitted spontaneously, by assuming a constant average gain per pass g . An elementary

calculation yields when $N \gg 1$ and $g \ll 1$, $P_N/P_0 = N - 1 + (1 + g)^N \approx N + \exp(gN)$. Clearly when $gN \gg 1$ the result is very sensitive to small changes in g and N . If one takes the experimental values corresponding to the maximum observed final power of $P_N = 2.7 \times 10^7$ W within the resonator, $N = 540$ and the computed spontaneous power of $P_0 = 6.5 \times 10^{-2}$ W, one finds that $g = 0.037$. The experimental value of linear gain is 0.067. In view of the sensitivity to changes in N and g the results are not inconsistent. Moreover this effective value of g is smaller than the linear gain predicted by the present model which is reasonable since non-linear effects and initial beam thermal effects must lower the gain. Unfortunately the currently available data is inadequate to make other detailed comparisons with this small-signal theory.

Our analysis suggests possible ways to substantially shorten the oscillator start-up time while maintaining high saturated power levels. The first approach takes advantage of the fact that the maximum linear gain and maximum saturated power occur for different values of δL , which we will respectively denote by δL_1 and δL_2 . By slightly increasing the frequency of the R.F. accelerating field, ω_{acc} , during the start-up period, i.e., decreasing the beam pulse separation, the value of δL , could be varied from an initial value of δL_1 to the value of δL_2 , thus, decreasing the start-up time while maintaining high final power levels. The required fractional increase in ω_{acc} is $|\delta L_1 - \delta L_2|/L_b \approx 10^{-6}$ for the parameters of Ref. 3 and 4. The same effect may also be realized by simply changing (increasing) the mirror separation during the start-up period. Another possible method of decreasing the start-up time would be to simply increase that part of F_{inc} associated with mirror losses, i.e., increase f_m . This could be accomplished by increasing the effective size of the mirror located at $z = L$. The additional extension of the mirror would necessarily have a different curvature. This last approach should make it possible to contain a far larger portion of the incoherent radiation.

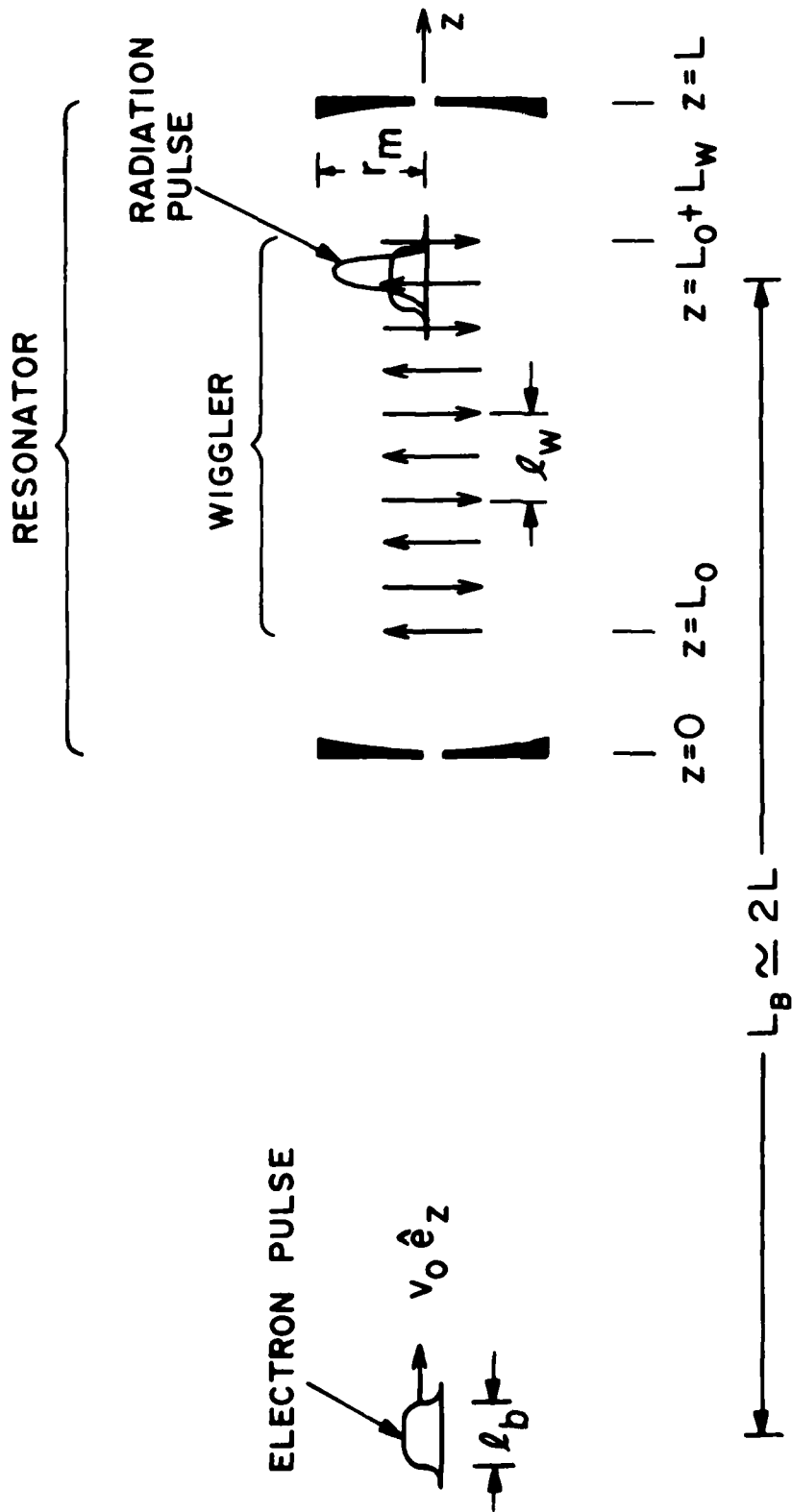


Fig. 1 Schematic of the pulsed electron beam FEL oscillator model.

Table I: FEL Oscillator Parameters at Stanford University

Beam Parameters

| | |
|---------------------------------------|---------|
| Beam Energy, $(\gamma_0 - 1) m_0 c^2$ | 43 MeV |
| Total Gamma, γ_0 | 85 |
| Axial Gamma, γ_{0z} | 69 |
| Peak Current, I_p | 1.3 A |
| Pulse Width, ℓ_b | 1 mm |
| Pulse Separation, L_b | 25.4 m |
| Beam Radius, r_b | 0.25 mm |

Wiggler Parameters

| | |
|--------------------------------------------------------|--------|
| Wiggler Wavelength, ℓ_w | 3.3 cm |
| Wiggler Amplitude (helical), $B_w = 2\pi A_w / \ell_w$ | 2.3 kG |
| Wiggler Length, L_w | 5.3 m |

Resonator and Radiation Parameters

| | |
|------------------------------------------|-------------------|
| Resonator Length, L | 12.7 m |
| Resonator Losses (round trip) | 1.5% |
| Radiation Wavelength, λ_L | 3.3 μm |
| Spot Size, r_0 | 0.167 cm |
| Beam Filling Factor, F_c | 0.017 |
| Incoh. Rad. Loss Factor, f_m | 0.05 |
| Rayleigh Length, $\pi r_0^2 / \lambda_L$ | 2.71 m |

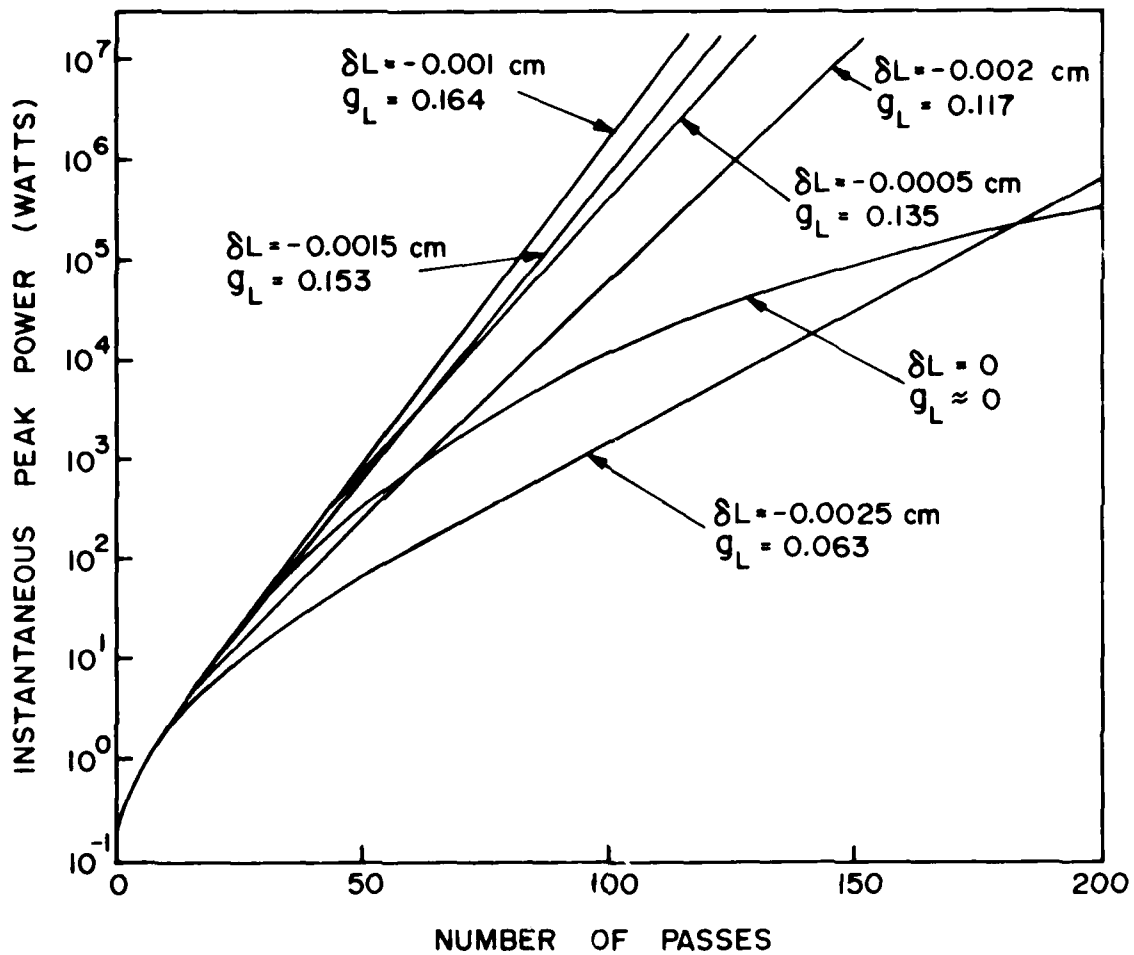


Fig. 2 Peak power of the radiation pulse as a function of the number of passes for Stanford FEL oscillator experiment with various detuning parameters δL .

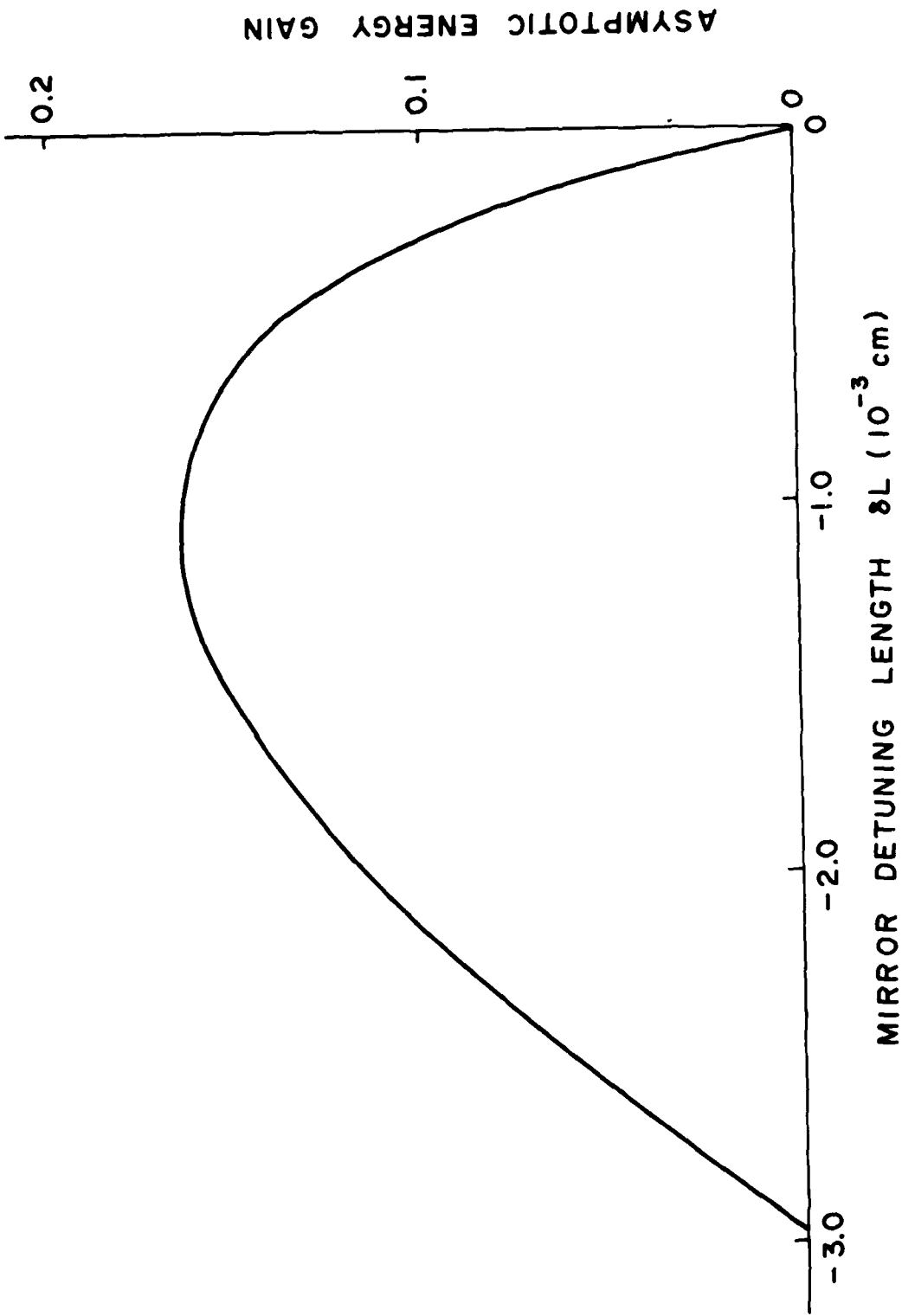


Fig. 3 Asymptotic energy gain ($t_N \gg 2L/v_{z0}$) of the radiation pulse as a function of δL for the Stanford FEL oscillator experiment.

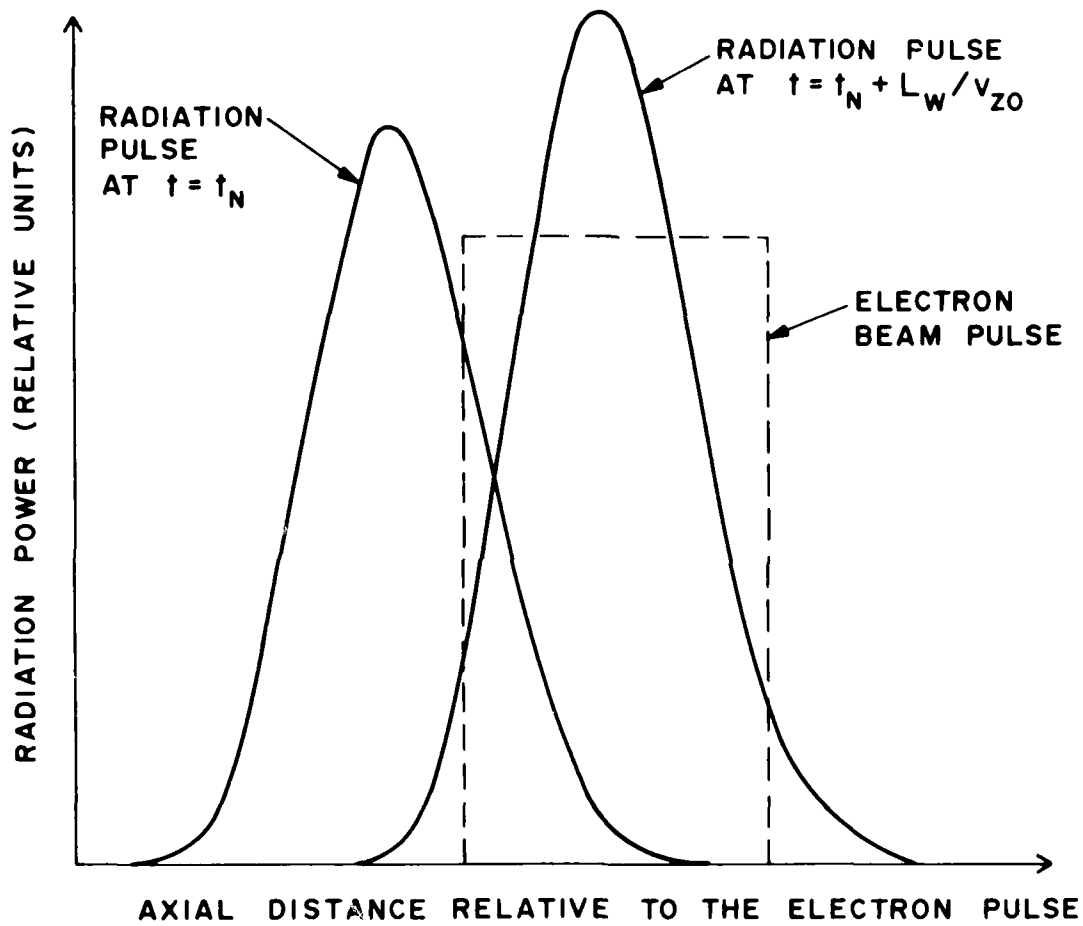


Fig. 4 Radiation pulse power relative to the spatial profile of the electron pulse (square) at the entrance of the wiggler ($t = t_N$) and exit of wiggler ($t = t_N + L_w/v_{z0}$), where $N \gg 1$ denotes the electron pulse number for the Stanford FEL oscillator experiment with $\delta L = -1.0 \times 10^{-3}$ cm.

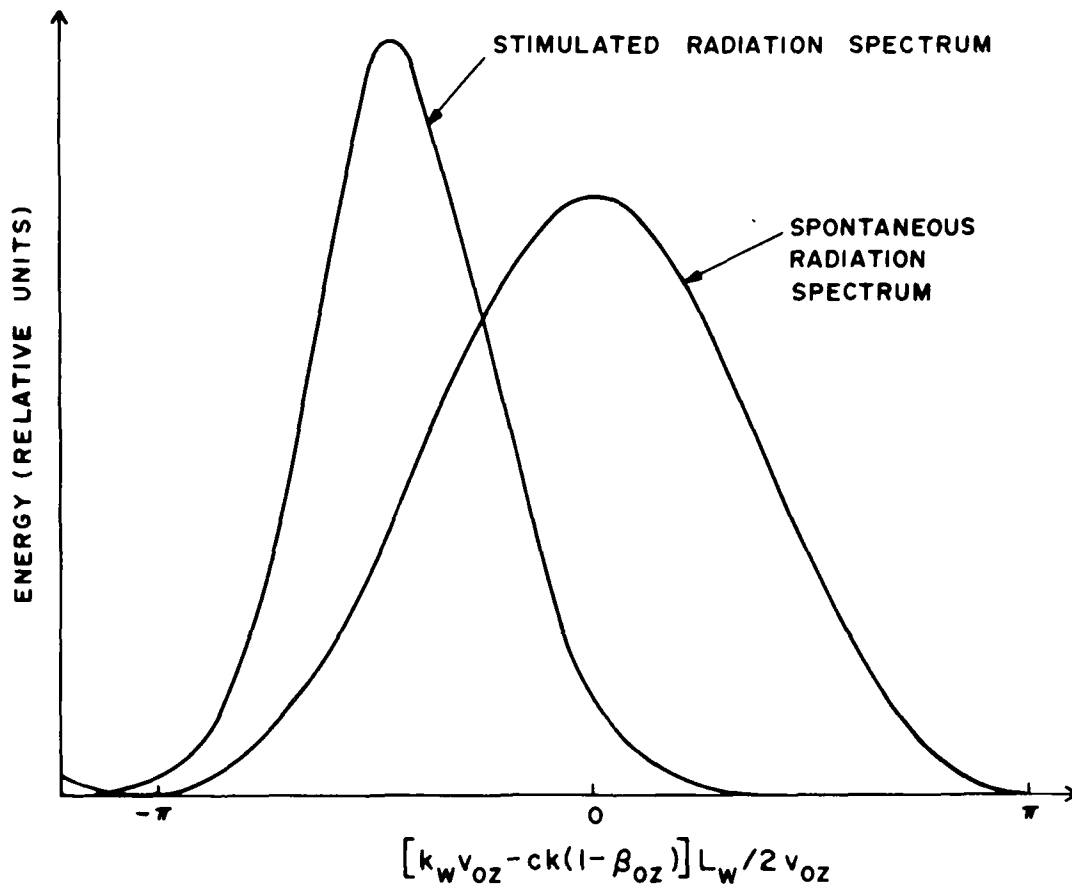


Fig. 5 Asymptotic energy spectrum of the radiation pulse for the Stanford FEL oscillator experiment with $\delta L = -1.0 \times 10^{-3}$ cm.

Acknowledgment

The authors are grateful to Dr. W. Colson for many illuminating discussions. This work was supported by DARPA under contract No. 3817.

References

1. D. A. G. Deacon, L. R. Elias, J. M. J. Madey, G. J. Ramian, H. A. Schwettman and T. I. Smith, Phys. Rev. Lett. 38, 892 (1977).
2. J. M. J. Madey, et al., Final Technical Report to ERDA, Contracts FY-76-03-0326 PA 48 and PA 49 (1977).
3. J. N. Eckstein, J. M. J. Madey, D. A. G. Deacon, T. I. Smith, S. Benson and A. Gaupp, Physics of Quantum Electronics, Vol 8, Chap. 2, ed. Jacobs, Pilloff, Scully, Moore, Sargent and Spitzer, Addison-Wesley, Reading, MA, 49 (1982).
4. S. Benson, D. A. G. Deacon, J. N. Eckstein, J. M. J. Madey, K. Robinson, T. I. Smith and R. Taber, to be published in the Proceedings of Bendor Free Electron Laser Conference, Bendor, France, Sep 27-Oct 1, 1982.
5. H. Al-Abawi, F. A. Hopf, G. T. Moore and M. O. Scully, Optics Comm. 20, 235 (1979).
6. G. T. Moore, M. O. Scully, F. A. Hopf and P. Meystre, Proc. Intl. School of Phys. E. Fermi, Course LXXIV, ed. C. Pellegrini, "Developments in High Power Lasers and Their Applications", North-Holland, Holland, 385 (1981).
7. F. A. Hopf, T. G. Kuper, G. T. Moore and M. O. Scully, Free-Electron Generators of Coherent Radiation, Physics of Quantum Electronics, Vol. 7, Chap 3, ed. Jacobs, Pilloff, Sargent, Scully and Spitzer, Addison-Wesley, Reading, MA, 31 (1980).
8. T. G. Kuper, G. T. Moore and M. O. Scully, Optics Comm. 34, 117 (1980).
9. G. T. Moore and M. O. Scully: Phys. Rev. A21, 2000 (1981).
10. W. B. Colson and S. K. Ride, Phys. Lett. 79A, 379 (1980).
11. W. B. Colson and S. K. Ride, Vol 7, Ref. 7, Chap. 13, 57 (1980).
12. W. B. Colson, Intl. School of Quantum Electronics, Erice (Italy), 1980.
13. W. B. Colson, Vol. 8, Ref. 3, Chap. 19, 457 (1982).

14. J. C. Goldstein and W. B. Colson, Proceedings of the 1981 International Conf. on Lasers (Laser '81), New Orleans, 93 (1981).
15. G. Dattoli, A. Marino and A. Renieri, Optics Comm., 35, 407 (1980).
16. G. Dattoli, A. Marino, A. Renieri and F. Romanelli, IEEE J. of Quantum Electronics, QE-17, 1371 (1981).
17. G. Dattoli and A. Renieri, Nuovo Cimento 61B, 153 (1981).
18. G. Dattoli and A. Marino and A. Reniero, Vol 8, Ref. 3, Chap. 22, 531 (1982).
19. W. B. Colson and A. Renieri, to be published in the Proceedings of Bendor Free Electron Laser Conference, Bendor, France, Sept 27-Oct 1, 1982.
20. B. N. Moore, M. N. Rosenbluth and H. V. Wong, Austin Research Associates Report I-ARA-72-U-89, 1982.
21. N. M. Kroll and W. A. McMullin, Phys. Rev. A17, 300 (1978).
22. W. B. Colson, Phys. Lett. A64, 190 (1977).
23. T. Kwan, J. M. Dawson and A. T. Lin, Phys. Fluid 20, 581 (1977).
24. P. Sprangle, R. A. Smith and V. L. Granatstein, Infrared and Millimeter Waves, Vol. 1, Edited by K. Button (Academic Press, New York) 1979.
25. N. M. Kroll, P. L. Morton and M. N. Rosenbluth, Vol. 7, Ref. 3, Chap. 4, 89 (1980).
26. P. Sprangle, C. M. Tang and W. M. Manheimer, Phys. Rev. A21, 302 (1980).
27. N. M. Kroll, P. L. Morton and M. N. Rosenbulth, IEEE J. of Quantum Electronic, QE-17, 1436 (1981).
28. P. Sprangle and C. M. Tang, Appl. Phys. Lett. 39, 677 (1981) and C. M. Tang and P. Sprangle, Chap. 27, Vol 9, Ref. 3, 627 (1982).
29. P. Sprangle, C. M. Tang and I. B. Bernstein, NRL Memorandum Report 5011 (1983).
30. J. D. Jackson, Classical Electrodynamics, John Wiley and Sons, Inc., New York, 1975.

**ATE
LMED**